Progress In Electromagnetics Research M, Vol. 106, 215–226, 2021

A Compact Dual Notch-Band Frequency Reconfigurable UWB Monopole Antenna

Jing-Chang Nan, Jiu-Yang Zhao*, and Yuan Wang

Abstract—To meet the requirements of miniaturization, multi-functions, and anti-interference of the antenna, this paper proposes a compact dual notch band frequency reconfigurable ultra-wideband (UWB) antenna. The antenna consists of an angle-cut rectangular radiation patch, a coplanar waveguide (CPW) structure, and a defective ground structure (DGS). A C-slot and an inverted U-slot are introduced to eliminate the interference of the Indian National Satellite band (INSAT), 5G band, and X satellite communication band. By controlling the PIN diodes across the two slots, the antenna can work in four states: UWB, two single notch bands, and one dual notch band. The impedance bandwidth in UWB mode is 2.9–12 GHz, with a relative bandwidth of 122%. The notch frequencies are 4.2–5.2 GHz and 6.2–8.1 GHz, respectively. In the passband of the antenna, the maximum gain is 7.17 dBi, and the group delay is less than 1 ns. The antenna size is $18 \times 17 \times 1.6\,\text{mm}^3$, which is easy to integrate with the communication systems. The antenna can be freely switched between the UWB mode and each notch band mode, which can be applied to the UWB wireless communication systems.

1. INTRODUCTION

In 2002, the Federal Communications Commission (FCC) passed a bill to apply ultra-wideband (UWB: 3.1–10.6 GHz) technology for commercial applications [1]. After that, UWB technology has been used in intelligent transportation systems, Internet of Things, and other fields because of its large system capacity, wide spectrum bandwidth, high transmission rate, low transmission power, and high communication security [1, 2]. With the increasing demand for miniaturization, portability, and multifunctionality of devices, microstrip antennas are commonly used due to their light weight, low profile, small size, easy integration, and low cost [3]. To improve the antenna gain and impedance bandwidth, planar monopole structures [4], defective ground structure (DGS) [5], fractal structures [6], electromagnetic band-gap (EBG) structure, and coplanar waveguide (CPW) feeding techniques [7, 8] have been widely used for the miniaturized design of UWB antennas.

However, it is still a challenge to design UWB antennas with optimal characteristics, because the large bandwidth of UWB technology leads to the overlap of communication bands between UWB systems and many narrowband communication systems, which in turn causes mutual interference between communications [9]. These narrowband communication systems include the Indian national satellite band (INSAT 4.5–4.8 GHz) and the X satellite communication band (7.25–7.75 GHz) [10]. Therefore, it is particularly important to design a notch UWB antenna with anti-interference performance, stable gain, omnidirectional radiation pattern, and wide impedance bandwidth [11]. To eliminate the interference of the narrowband communication system to the UWB system, the narrowband notch is designed without affecting the required characteristics of the UWB antenna. There are many ways to achieve notch, such as loading short cut lines [5], surface slots [12–14], loading split-ring resonator (SRR) [15, 16], complementary split-ring resonator (CSRR) [17], and loading parasitic elements on the

Received 8 September 2021, Accepted 20 December 2021, Scheduled 28 December 2021
* Corresponding author: Jiu-Yang Zhao (zhaojiuyang2020@163.com).
The authors are with the School of Electronics and Information Engineering, Liaoning Technical University, Huludao 125105, China.

antenna [18]. In [19], a planar UWB antenna with tri-band notch characteristics was proposed. The notch characteristics of the antenna in WiMAX, WLAN, and X satellite communication bands were realized by etching circular and C-shaped slots on the radiation patch and ground. Reference [20] proposed a dual notch printed monopole UWB antenna fed by CPW, which used a rectangular slot to realize the notch of WLAN and X band satellite communication.

Band-notched UWB antenna can solve the interference problem of narrowband communication, but the notch frequency is fixed, and the interference does not always exist. Therefore, it is necessary to design a band-notched reconfigurable UWB antenna that can reject interference and maximize the advantages of UWB antenna. Commonly used reconfigurable methods are adding FET switches [21, 22], MEMS switches [23, 24], varactor diodes [25, 26], and PIN diodes [27–31] to the antenna. PIN diodes are often used for RF switching due to their small switching losses, good stability, low price, and easy control. In [24], a dual-band notch reconfigurable CPW-fed circular monopole UWB antenna based on a silicon substrate was proposed. RF MEMS SP4T switch was used to realize the reconfiguration of the antenna across two slots of the radiation patch. In [25], a tunable filter UWB antenna fed by CPW was proposed. The antenna used an adjustable resonator to realize the notch band. By introducing a variable capacitance on the resonator, the capacitance value was changed to adjust the notch band. Reference [27] proposed a DGS structure to improve the working bandwidth and impedance matching of the antenna and applied a slot-type split-ring resonator (ST-SRR) structure to the feed line to achieve band-notched characteristics. The PIN diode was inserted into the ST-SRR structure to realize the frequency band reconfiguration of the antenna. However, the size of the above antenna is relatively large, and the structure is complicated.

In this paper, the miniaturization, anti-interference, and multi-functional requirements of the antenna are comprehensively considered. For INSAT band, X satellite communication band, and other applications, a reconfigurable UWB antenna with -10 dB impedance bandwidth of 2.9–12 GHz is proposed. By controlling the state of PIN diode switches on different slots, UWB and different notch band modes are realized. Finally, the simulated and measured results will be discussed below.

2. ANTENNA DESIGN

2.1. Antenna Structure

The antenna structure and parameters are shown in Figure 1. The antenna designed in this paper is printed on an F4B ($\varepsilon_r = 2.55$, $\tan\delta = 0.002$) dielectric substrate with the size of $18 \times 17 \times 1.6\,\text{mm}^3$. The antenna uses a CPW structure with a cut-angle rectangular radiating patch and a cut-angle ground plate for extending the antenna bandwidth. The C-shaped slot of the radiation patch is used to realize the INSAT band notch. The inverted U-shaped slot at the feed line is to realize the X band notch. The reconfigurable antenna is achieved by connecting PIN diode switches to the C-shaped slot and inverted U-shaped slot. The optimized antenna structure parameters are as follows: $W = 18$ mm, $L = 17$ mm,

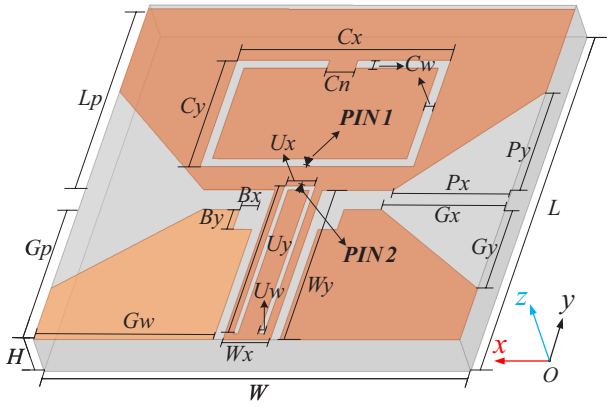

Figure 1. The proposed antenna structure and parameters.

$H = 1.6\,\text{mm}$, $Gw = 7.6\,\text{mm}$, $Gp = 6.6\,\text{mm}$, $Lp = 9.2\,\text{mm}$, $Gx = 5.2\,\text{mm}$, $Gy = 4\,\text{mm}$, $Uw = 0.2\,\text{mm}$, $Bx = 0.8\,\text{mm}$, $By = 1\,\text{mm}$, $Cw = 0.4\,\text{mm}$, $Px = 5\,\text{mm}$, $Py = 5\,\text{mm}$, $Cn = 1.2\,\text{mm}$, $Wx = 2\,\text{mm}$, $Wy = 7.6\,\text{mm}$, $Cy = 5.4\,\text{mm}$, $Ux = 1.3\,\text{mm}$, $Uy = 7.5\,\text{mm}$, and $Cx = 9\,\text{mm}$.

2.2. Notch Principle of Antenna

The notch principle of the antenna is to make the notch structure length about half of the wavelength at the notch center frequency. The antenna will resonate at the notch frequency band, resulting in the opposite directions of current flows on the two sides of the slot, and electromagnetic waves in the notch band cannot be radiated and received normally. In this paper, the C-slot and inverted U-slot structures are introduced, and by adjusting the size and location of the slots, the INSAT and X band notch are formed. The approximate size of each slot can be calculated by the following equations:

$$L_{\text{notch}} = \frac{c}{2f_{\text{notch}}\sqrt{\varepsilon_{eff}}} \tag{1}$$

$$\varepsilon_{eff} = \frac{\varepsilon_r + 1}{2} + \frac{\varepsilon_r - 1}{2}\left(1 + \frac{12h}{w_x}\right)^{-0.5} \tag{2}$$

where L_{notch} is the slot length, f_{notch} the notch center frequency, ε_r the dielectric constant of substrate, ε_{eff} the effective dielectric constant, c the speed of light, h the substrate thickness, and w_x the feed line width.

2.3. Reconfigurable Principle of Antenna

Two PIN diodes are connected to the appropriate position of two slots. The on/off state of diodes is controlled by the bias circuit. Different diode states change the structure of slots, which in turn changes the antenna current distribution and produces the antenna multifunctional characteristics. In this paper, the MA4AGBLP912 PIN diode of the M/A-COM company is selected. From the datasheet of PIN diode [32], the PIN diode has low forward conduction resistance and inductance, and large reverse resistance. The applicable frequency band of the diode is up to 40 GHz, which meets the requirements of the antenna designed in this paper. The equivalent circuit model of the diode is established according to the datasheet. When the diode is on, the inductor ($L_s = 0.5\,\text{nH}$) is connected in series with the resistor ($R_s = 4\,\Omega$), which makes the current pass through the diode smoothly. When the diode is off, the capacitor ($C_p = 0.026\,\text{pF}$) is paralleled with the resistor ($R_p = 10\,\text{k}\Omega$), and then in series with the inductor ($L_s = 0.5\,\text{nH}$) to prevent the current from passing through the diode. The diode equivalent circuits are shown in Figure 2.

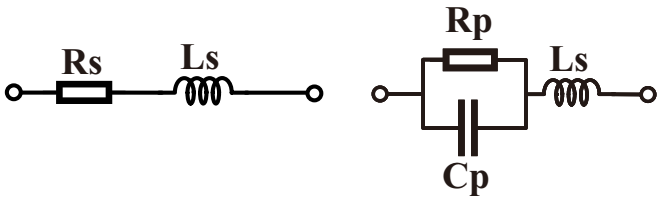

Figure 2. Equivalent circuit of diode switch in different states, (a) diode on, (b) diode off.

2.4. Design Process of Antenna

Figure 3 shows the design process of the reconfigurable antenna and bandwidth characteristics analysis. From Figure 3, we can see that structure 1 adopts a rectangular radiation patch, DGS, and CPW structure, but it does not meet the design requirements at the low frequency band. Structure 2 cuts the angles of the radiation patch and ground plane, which improves antenna bandwidth, and the passband has met the requirements of UWB antenna. To reject the mutual interference between communication

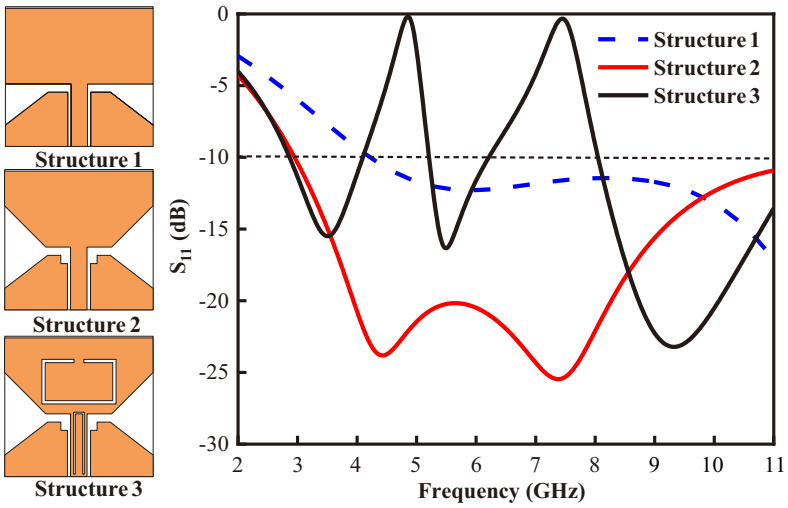

Figure 3. Antenna design process and bandwidth characteristics analysis.

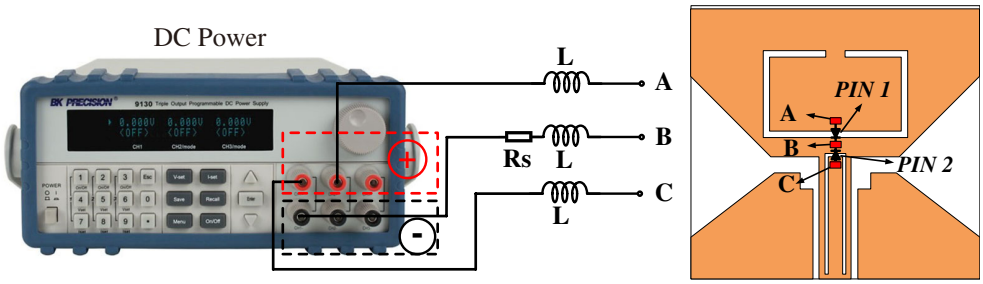

(a)

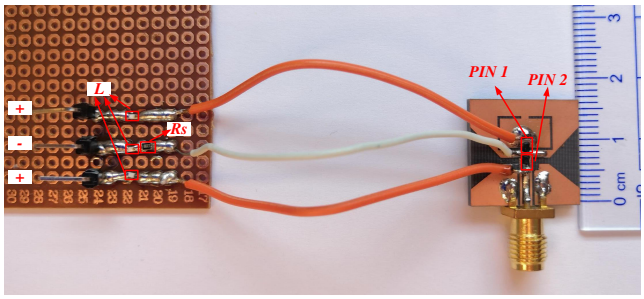

(b)

Figure 4. Bias circuit, (a) schematic diagram, (b) fabricated prototype.

systems, a C-shaped slot and an inverted U-shaped slot are introduced in structure 3, and the slots produce INSAT band notch and X satellite communication band notch.

To realize the multi-functional characteristics of the antenna and make full use of the spectrum resources, PIN diode switches are connected at the C-shaped slot and inverted U-shaped slot. The reconfigurable characteristics of the antenna are realized by controlling the on/off state of diode switches at different positions through external circuit. To control the state of PIN diodes, the bias circuit needs to be designed. To avoid circuit complexity, common ground connection is used. In the bias circuit, A and B are connected across the two ends of the C-slot, and B and C are connected across the two sides of the inverted U-slot. To prevent the instability of power source caused by RF signal through the bias circuit, the inductor ($L = 30\,\text{nH}$) is used at the bias circuit to suppress the RF signal. The

220 Ω resistance is used to limit the current through the diode and to protect the circuit. The schematic diagram and fabricated prototype of the bias circuit are shown in Figure 4.

Figure 5 is the antenna design flowchart. Firstly, we designed a simple rectangular patch antenna to meet the UWB requirements by optimizing the parameters of the radiation patch and ground floor. Then, the C-shaped slot and inverted U-shaped slot are etched in the antenna. By optimizing the relevant parameters of the slot structure, the antenna forms the notch in the INSAT frequency band and X satellite communication band. Finally, to make the antenna multi-functional, two PIN diodes are added to the slot structures of the antenna, and the bias circuit is designed to control the switching state of different diodes to form four working modes of the antenna.

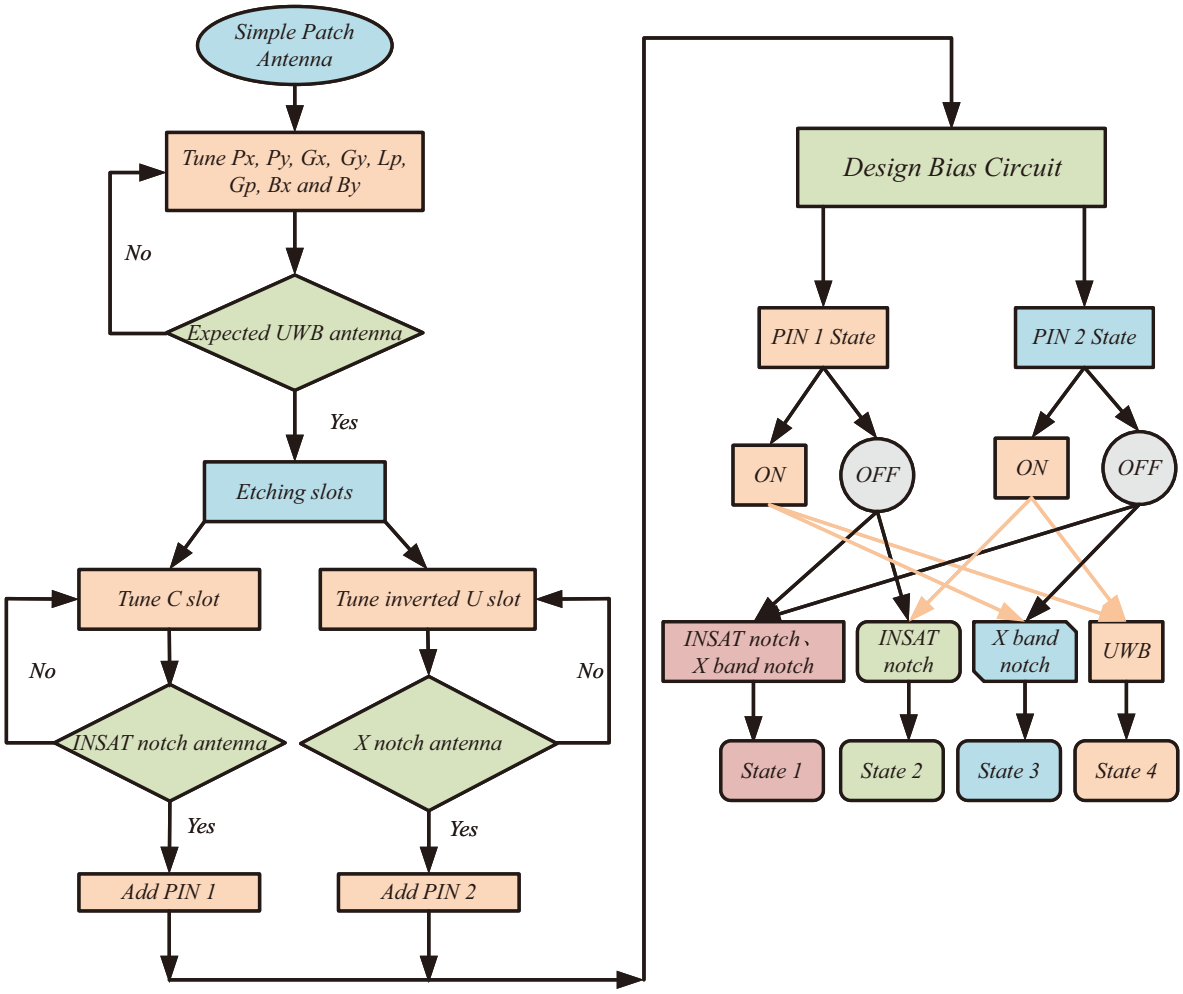

Figure 5. Design procedure of the proposed antenna with reconfigurable characteristics.

2.5. Analysis of Notch Frequency Band

Figure 6 shows the influence of notch structure parameters on antenna reflection coefficient. C_y and U_y are the key parameters of C-shaped slot and inverted U-shaped slot, respectively. The figure shows that with the increase of C_y and U_y length, the notch center frequency moves to the low frequency direction, which also verifies the inverse relationship between the notch center frequency and the notch branch length in Equation (1). From the principle of notch, by changing the length of notch branch, the notch can be formed in any frequency band. However, in actual design, it is found that different notch structures will affect each other, which makes the design of multiple notch antennas very difficult.

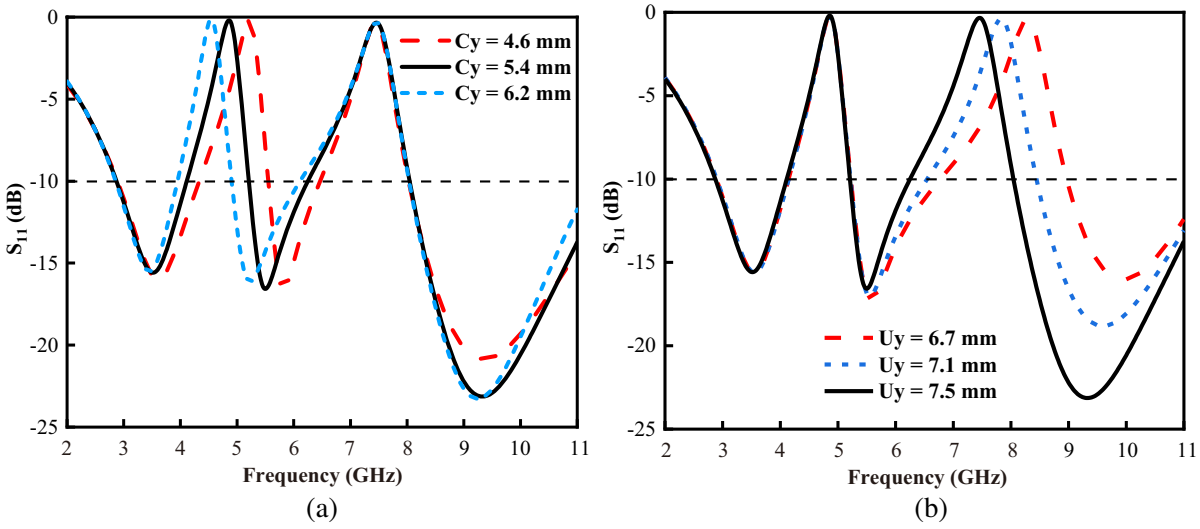

Figure 6. The influence of notch structure parameters on antenna reflection coefficient. (a) S_{11} with different C_y, (b) S_{11} with different U_y.

2.6. Current Distribution on Antenna Surface

Figure 7 shows the antenna surface current distribution. In Figure 7(a), the current is mainly concentrated around the C-slot at the notch frequency of 4.7 GHz. In Figure 7(b), the surface current at the notch frequency of 7.5 GHz is mainly concentrated around the inverted U-slot. The current flow directions on the two sides of the slot are opposite so that the electromagnetic field generated by the antenna cannot be effectively radiated. The opposite currents lead to low gain, low radiation efficiency, and forms notch. Due to the mutual anisotropy of antennas, the notch frequency band cannot effectively receive the electromagnetic wave, which in turn suppresses the interference of narrowband signals on the UWB system.

When the diode loaded at the slot is on, the current passes through the diode, which changes the original current distribution, and then changes the notch characteristics of the antenna. In Figure 7(c),

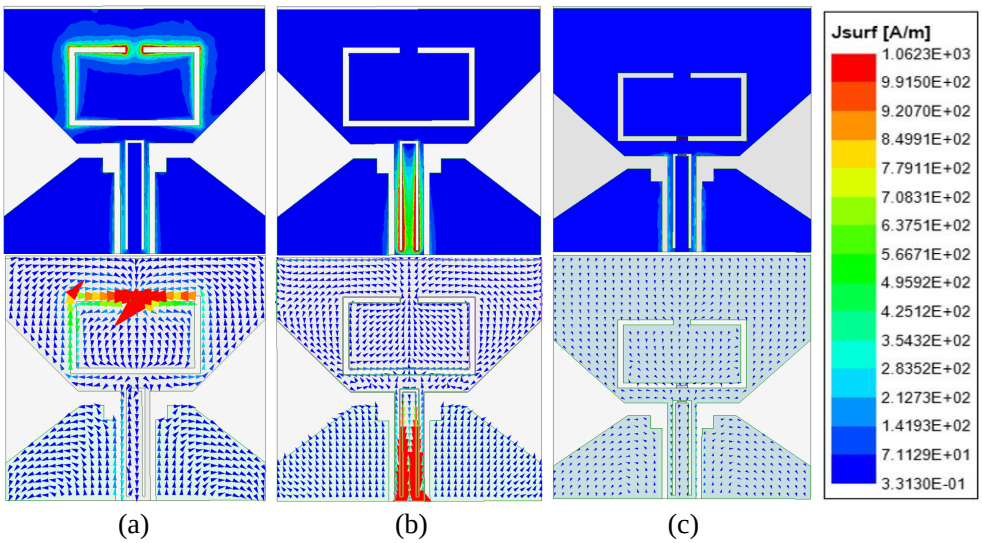

Figure 7. Surface current distribution of the antenna. (a) Current at 4.7 GHz, (b) current at 7.5 GHz, (c) current when diode is on.

when the diode switch is on, at the central frequency of the notch, the current is not concentrated around the slot, and the slot inner and outer currents are in the same direction. The electromagnetic wave can normally radiate, so the notch characteristics disappear.

3. EXPERIMENTAL RESULTS AND DISCUSSION

3.1. *S* Parameter of the Antenna

Using Keysight E5063A vector network analyzer to measure the S parameters of the antenna. Figure 8 is the comparison result of the simulated and measured S parameters. The experimental results show that in state 1, two PIN diodes are turned off, and the antenna works in dual-notch mode. In state 1, the antenna generates notches at 4.2–5.2 GHz and 6.2–8.1 GHz, which can suppress the interference of the INSAT band (4.50–4.80 GHz) and X band (7.25–7.75 GHz). In state 2, only PIN 2 is turned on, and the antenna works in INSAT notch mode. In state 3, only PIN 1 is turned on, and the antenna works in X band notch mode. In state 4, two PIN diodes are turned on, and both notch structures are destroyed, which cannot form notches, and the antenna works in UWB mode. Thus, the variation of the PIN diode switching state provides reconfigurability between the notch bands in the UWB systems. Antenna modes under different PIN switching states are shown in Table 1.

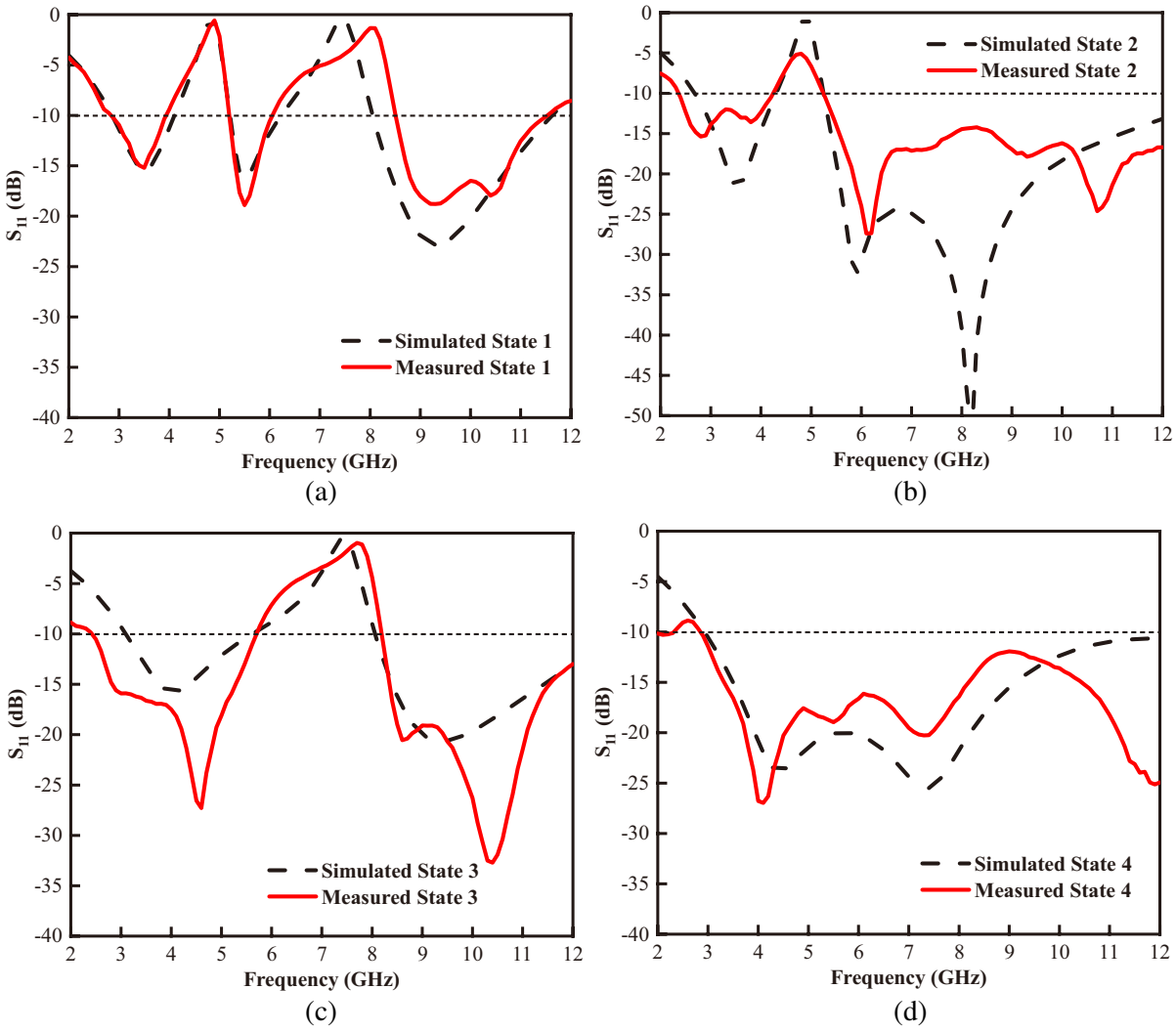

Figure 8. Comparison of S parameter simulation and measurement of antenna. (a) State 1. (b) State 2. (c) State 3. (d) State 4.

Table 1. Antenna modes under different PIN switching states.

Modes	PIN 1	PIN 2	Antenna Application
State 1	OFF	OFF	INSAT notch, X band notch
State 2	OFF	ON	INSAT notch
State 3	ON	OFF	X band notch
State 4	ON	ON	UWB

3.2. Radiation Patterns of Antenna

Figure 9 shows the radiation patterns at 5.5 GHz, 9 GHz, and 10 GHz of the E-plane (xoy) and H-plane (xoz). The far-field radiation patterns are measured in an anechoic chamber. It can be seen that the radiation pattern of the antenna on the E-plane is the bidirectional radiation of the "8" shape, and the radiation pattern on the H-plane is omnidirectional radiation, which meets the requirements of the UWB monopole antenna. However, as the frequency increases, higher-order modes are generated and cause uneven phase distribution of the antenna, resulting in deterioration of the antenna radiation pattern.

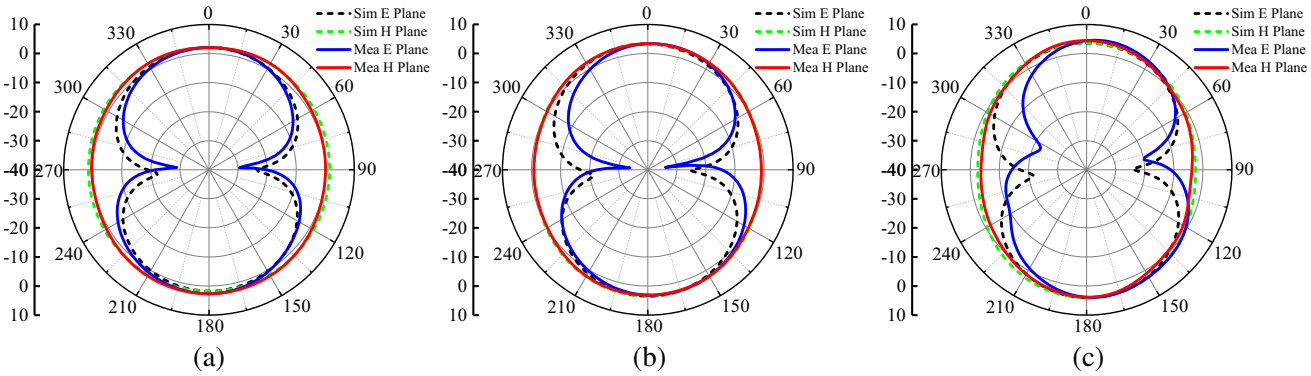

Figure 9. Antenna radiation patterns. (a) 5.5 GHz, (b) 9 GHz, (c) 10 GHz.

3.3. Antenna Gain

Figure 10(a) shows the gain of the antenna at state 1 (dual band notch). It can be seen that the gain in the notch band decreases significantly, and the antenna cannot radiate effectively in the notch band, which proves the effectiveness of the notch structure. The gain of the antenna is stable at about 4 dBi in the passband, and the maximum gain is 7.17 dBi, which can meet the application requirements of a UWB communication system.

3.4. Group Delay of Antenna

Figure 10(b) is the time domain analysis of the antenna. The group delay is measured by using two same antennas face-to-face with a distance of 20 cm. The system distortion can be ignored when the group delay is less than 1 ns [31]. In Figure 10(b), the group delay changes dramatically due to the antenna impedance mismatch at the notch frequency. The group delay of the proposed antenna in the passband is basically stable at about 1 ns, indicating that the antenna has good transmission characteristics.

3.5. Antenna Efficiency

Figure 11(a) and Figure 11(b) are the simulated and measured efficiency diagrams of the antenna under different switching states. To simulate the RF devices loaded with PIN diodes, it is necessary to use different circuit models for equivalent substitution of PIN diodes in different states, as shown in Figure 2. In Figure 11, we can see that the measured antenna efficiency is lower than the simulated one, and the difference between the measured and simulated efficiencies may come from the fabrication error of the diode switch and the parasitic effect of the diode. Although the measured antenna efficiency is not as high as the simulated one, the measured antenna efficiency in the passband is basically maintained at 80%. The simulated and measured results show that the efficiency of the antenna in the notch band is significantly reduced, and the notch band of the antenna in different modes meets the design requirements of the antenna.

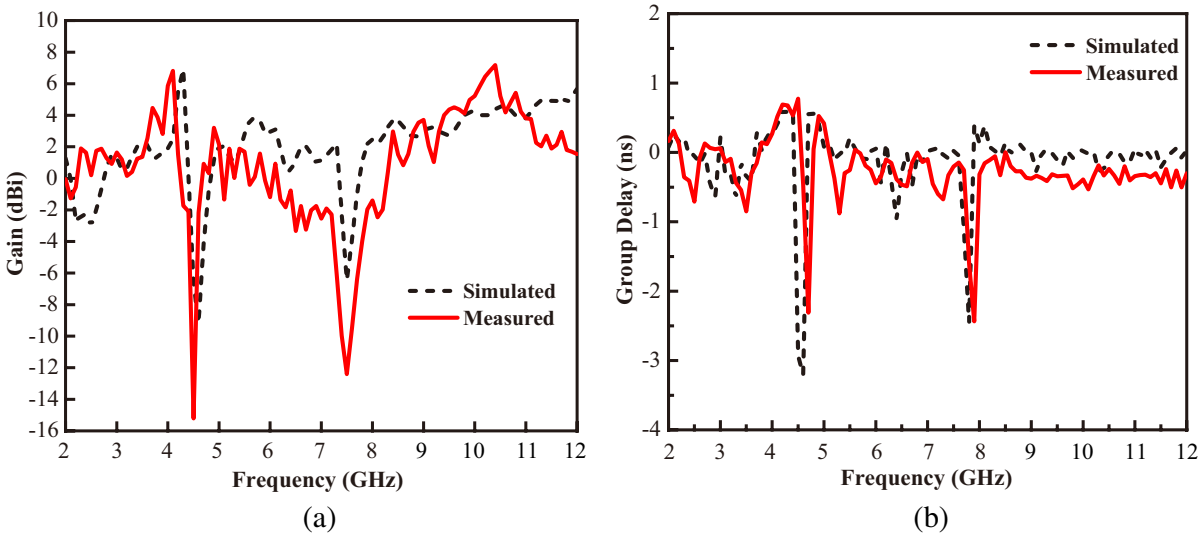

Figure 10. Gain and group delay of the antenna. (a) Gain, (b) group delay.

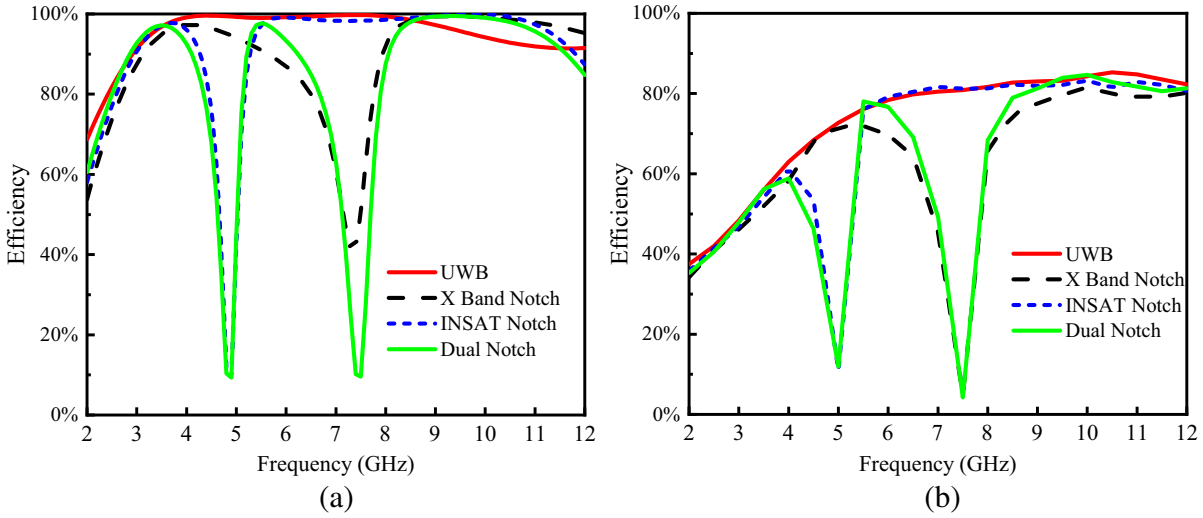

Figure 11. Antenna efficiency. (a) Simulated efficiency, (b) measured efficiency.

3.6. Comparison with Other Related Designs

Table 2 compares the proposed antenna with other related literature [24–30] in impedance bandwidth, switch type, antenna size, antenna mode, notch band, and applications. Compared with the antennas in [24–30], the antenna proposed in this paper has smaller size and more antenna states. The proposed antenna uses PIN diodes as a reconfigurable device, which has low cost, good performance, and wide application range.

Table 2. Comparison of antenna performance with other references.

Reference	Impedance Bandwidth (GHz)	Type of switch	Antenna size (mm^2)	mode	Notch frequency band (GHz)	Notch band Application
[24]	0.68–16.23	MEMS	47×47	4	3.33–3.76 and 4.92–6.14	WiMAX and WLAN
[25]	2.9–11	Variable capacitors	30.5×24	2	2.9–3.5 and 5.1–7	WiMAX and WLAN
[26]	2.7–10.6	Variable capacitors	31×30	2	2–3 and 3.2–4	WiMAX and WLAN
[27]	2.7–14.9	PIN	32×42	2	3.43–3.75 and 4.87–6.4	WiMAX and WLAN
[28]	2.6–10.7	PIN	35×41	3	3.5 and 5.5	WiMAX and WLAN
[29]	2.5–9.8	PIN and Varactor	36.6×26	2	4.2–4.8 and 5.8–6.5	C-band and WLAN
[30]	2.7–10.7	PIN	32×27	4	3.25–3.95 and 5.3–5.7	WiMAX and WLAN
This paper	2.9–12	PIN	18×17	4	4.2–5.2 and 6.2–8.1	INSAT, 5G and X band

4. CONCLUSIONS

A dual notch band frequency reconfigurable UWB antenna based on PIN diode is proposed. The reconfigurable characteristic of the antenna is to load PIN diode switches on both sides of the slot in the target frequency band. The bias circuit controls the on/off state of the diode, thus changing the antenna surface current distribution and radiation characteristics. The experiment results indicate that the antenna can work in four states, which can filter interference and improve spectrum utilization. Compared with the same type of UWB antenna, the proposed antenna size is smaller, which provides conditions for the integration of RF devices. In the passband, the maximum gain of the antenna is 7.17 dBi, the antenna efficiency maintained at 80%, and the group delay less than 1 ns, which indicates that the antenna can be applied to multi-functional and anti-interference UWB systems.

ACKNOWLEDGMENT

This work was supported by the National Natural Science Foundation of China (61971210).

REFERENCES

1. The Federal Communications Commission, "Revision of Part 15 of the Commission's rules regarding ultra-wideband transmission systems from 3.1 to 10.6 GHz," Federal Communications Commission, 98–153, Washington, DC, 2002.
2. Dong, J. and Q. Li, "Compact planar ultrawideband antennas with 3.5/5.2/5.8 GHz triple band-notched characteristics for internet of things applications," *Sensors*, Vol. 17, No. 2, 1–17, 2017.
3. Syed, A. and R. W. Aldhaheri, "A very compact and low profile UWB planar antenna with WLAN band rejection," *Scientific World Journal*, Vol. 2016, 1–7, 2016.

4. Jang, E. S., C. Y. Kim, D. G. Yang, and S. S. Hong, "Suppressed band characteristics of an UWB conical monopole antenna with split loops based on the equivalent circuit," *International Journal of Antennas and Propagation*, Vol. 2017, 1–8, 2017.
5. Borhani Kakhki, M. and P. Rezaei, "Reconfigurable microstrip slot antenna with DGS for UWB applications," *International Journal of Microwave and Wireless Technologies*, 1517–1522, 2017.
6. Rajkumar, S. and K. T. Selvan, "Compact 4 element Sierpinski Knopp fractal UWB MIMO antenna with dual band notch," *Microwave and Optical Technology Letters*, Vol. 60, 1023–1030, 2018.
7. Dalal, P. and S. K. Dhull, "Upper WLAN band notched UWB monopole antenna using compact two via slot electromagnetic band gap structure," *Progress In Electromagnetics Research C*, Vol. 100, 161–171, 2020.
8. Zhang, J., L. Wang, and W. Zhang, "A novel dual band-notched CPW-fed UWB MIMO antenna with mutual coupling reduction characteristics," *Progress In Electromagnetics Research Letters*, Vol. 90, 21–28, 2020.
9. Rahman, M. U. and J. D. Park, "The smallest form factor UWB antenna with quintuple rejection bands for IoT applications utilizing RSRR and RCSRR," *Sensors*, Vol. 18, No. 3, 1–16, 2018.
10. Oraizi, H. and N. V. Shahmirzadi, "Frequency- and time-domain analysis of a novel UWB reconfigurable microstrip slot antenna with switchable notched bands," *IET Microwaves, Antennas Propag.*, Vol. 11, No. 8, 1127–1132, 2017.
11. Kumar, G. and R. Kumar, "A survey on planar ultra-wideband antennas with band notch characteristics: Principle, design, and applications," *AEU — International Journal of Electronics and Communications*, Vol. 109, 76–98, 2019.
12. Iqbal, A., A. Smida, N. K. Mallat, M. T. Islam, and S. Kim, "A compact UWB antenna with independently controllable notch bands," *Sensors*, Vol. 19, No. 6, 1–12, 2019.
13. Hayouni, M., F. Choubani, et al., "Main effects ensured by symmetric circular slots etched on the radiating patch of a compact monopole antenna on the impedance bandwidth and radiation patterns," *Wireless Personal Communications*, Vol. 95, No. 4, 4243–4256, 2017.
14. Zhang, X.-Y., H. Xu, Y. Xie, and Q. Wu, "A dual band-notched antenna for UWB applications," *Progress In Electromagnetics Research Letters*, Vol. 96, 105–111, 2021.
15. Islam, M. T., F. Bin Ashraf, T. Alam, et al., "A compact ultrawideband antenna based on hexagonal split-ring resonator for pH sensor application," *Sensors*, Vol. 18, No. 9, 1–16, 2018.
16. Kaur, K., A. Kumar, and N. Sharma, "Split ring slot loaded compact CPW-fed printed monopole antennas for ultra-wideband applications with band notch characteristics," *Progress In Electromagnetics Research C*, Vol. 110, 39–54, 2021.
17. Dalal, P. and S. K. Dhull, "Design of triple band-notched UWB MIMO/diversity antenna using triple bandgap EBG structure," *Progress In Electromagnetics Research C*, Vol. 113, 197–209, 2021.
18. Yadav, D., M. P. Abegaonkar, S. K. Koul, V. Tiwari, and D. Bhatnagar, "A compact dual band-notched UWB circular monopole antenna with parasitic resonators," *AEU — International Journal of Electronics and Communications*, Vol. 84, 313–320, 2018.
19. Bakariya, P. S. and S. Dwari, "Triple band notch UWB printed monopole antenna with enhanced bandwidth," *AEU — International Journal of Electronics and Communications*, Vol. 69, 26–30, 2015.
20. Yadav, A. and D. Sethi, "Slot loaded UWB antenna: Dual band notched characteristics," *AEU — International Journal of Electronics and Communications*, Vol. 70, No. 3, 1–2, 2016.
21. Aboufoul, T., A. Alomainy, and C. Parini, "Reconfiguring UWB monopole antenna for cognitive radio applications using GaAs FET switches," *IEEE Antennas and Wireless Propagation Letters*, Vol. 11, 392–394, 2012.
22. Quddious, A., M. A. B. Abbasi, M. A. Antoniades, P. Vryonides, V. Fusco, and S. Nikolaou, "Dynamically reconfigurable UWB antenna using an FET Switch powered by wireless RF harvested energy," *IEEE Transactions on Antennas and Propagation*, Vol. 68, No. 8, 5872–5881, 2020.

23. Ibrahim, A. A., A. Batmanov, and E. P. Burte, "Design of reconfigurable antenna using RF MEMS switch for cognitive radio applications," *2017 Progress In Electromagnetics Research Symposium — Spring (PIERS)*, 369–376, St Petersburg, Russia, May 22–25, 2017.
24. Sharma, K., et al., "Reconfigurable dual notch band antenna on Si-substrate integrated with RF MEMS SP4T switch for GPS, 3G, 4G, bluetooth, UWB and close range radar applications," *AEU — International Journal of Electronics and Communications*, Vol. 110, 1–9, 2019.
25. Nejatijahromi, M., M. Naghshvarianjahromi, and M. Rahman, "Compact CPW fed switchable UWB antenna as an antenna filter at narrow-frequency bands," *Progress In Electromagnetics Research C*, Vol. 81, 199–209, 2018.
26. Nejatijahromi, M., M. Rahman, and M. Naghshvarianjahromi, "Continuously tunable WiMAX band-notched UWB antenna with fixed WLAN notched band," *Progress In Electromagnetics Research Letters*, Vol. 75, 97–103, 2018.
27. Lakrit, S., S. Das, A. El Alami, D. Barad, and S. Mohapatra, "A compact UWB monopole patch antenna with reconfigurable Band-notched characteristics for Wi-MAX and WLAN applications," *AEU — International Journal of Electronics and Communications*, Vol. 105, 106–115, 2019.
28. Yang, H., X. Xi, H. Hou, Y. Zhao, and Y. Yuan, "Design of reconfigurable monopole antenna with switchable dual band-notches for UWB applications," *International Journal of Microwave and Wireless Technologies*, Vol. 10, No. 9, 1065–1071, 2018.
29. Wu, W., Y. B. Li, R. Y. Wu, et al., "Band-notched UWB antenna with switchable and tunable performance," *International Journal of Antennas and Propagation*, Vol. 2016, 1–6, 2016.
30. Srivastava, G., S. Dwari, and B. K. Kanaujia, "A compact UWB antenna with reconfigurable dual notch bands," *Microwave and Optical Technology Letters*, Vol. 57, No. 12, 2737–2742, 2015.
31. Tripathi, S., A. Mohan, and S. Yadav, "A compact fractal UWB antenna with reconfigurable band notch functions," *Microwave and Optical Technology Letters*, Vol. 58, No. 3, 509–514, 2016.
32. M/A-COM Data Sheet for MA4AGBLP912 beam lead PIN diode.